Molecular Diversity
https://doi.org/10.1007/s11030-020-10086-2

ORIGINAL ARTICLE

Synthesis, computational study and cytotoxicity of 4-hydroxycoumarin-derived imines/enamines

Samaneh Vaseghi[1] · Mohammad Yousefi[2] · Mohammad Shokrzadeh[3] · Zinatossadat Hossaini[4] · Zahra Hosseini-khah[5] · Saeed Emami[6]

Received: 14 October 2019 / Accepted: 8 April 2020

Abstract

In this study, we applied a direct condensation between 3-acetyl-4-hydroxy-2*H*-chromen-2-one and different amines (anilines and benzyl amines) in order to synthesize some coumarin-based imines/enamines (**3a–o**) as cytotoxic agents. All the compounds were characterized by means of FT-IR, NMR, mass spectroscopy and elemental analyses. Since the title compounds can exist as different forms including (*s-cis*)-imine and (*s-trans*)-imine or (*E* and *Z*)-enamines, their conformational and geometrical aspects were investigated computationally by DFT method. The optimized geometry parameters, ΔE, ΔG, ΔH, Mulliken atomic charge, HOMO and LUMO energy, and NBO analysis suggested that these compounds can exist predominantly in (*E*)-enamine form. All the synthesized compounds (**3a–o**) were evaluated in vitro for their cytotoxic activities against cancer cell lines (MCF-7 and A549) and normal cell line (BEAS-2B) using the MTT assay. The 4-hydroxybenzyl derivative **3k** was found to be the most potent cytotoxic agent with no selectivity, similar to doxorubicin. However, the 4-chlorobenzyl analog **3o** could be considered as an equipotent compound respect to doxorubicin with higher selectivity.

Graphic abstract

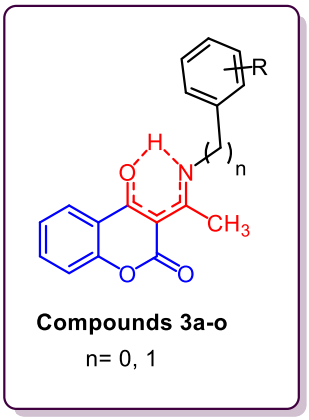

Keywords Anticancer · 2*H*-chromen-2-one · Coumarin · Schiff bases · Computational study · DFT

Introduction

According to World Health Organization (WHO) reports, cancers will cause more than 13 million deaths in 2030. These reports also indicate that 20% of people under age 75 will struggle with cancer in their lifetime [1, 2]. Nowadays, chemotherapy is the essential approach for the cancer

Electronic supplementary material The online version of this article (https://doi.org/10.1007/s11030-020-10086-2) contains supplementary material, which is available to authorized users.

✉ Saeed Emami
sdemami12@gmail.com; semami@mazums.ac.ir

Extended author information available on the last page of the article

Published online: 22 April 2020

treatment [3], even though it faces disadvantages such as drug resistance and drug-induced toxicity [4, 5]. In this situation, finding new anticancer agents with high potency and proper therapeutic index is urgently required.

Chromone derivatives including coumarin (2*H*-chromen-2-one, 2*H*-1-benzopyran-2-one) ones possess unique biological properties such as anti-inflammatory [6], antioxidant [7], antinociceptive [8], hepatoprotective [9], antithrombotic [10, 11], antiviral [12, 13], antimicrobial [14, 15], antituberculosis [16], anti-carcinogenic [17], antihyperlipidemic [18] and anticholinesterase [19] activity. Therefore, applying coumarin backbone to synthesize novel derivatives for further screening as novel therapeutic agents is the driving force for diverse investigations.

Among coumarin derivatives, 4-hydroxycoumarin analogs and complexes can inhibit cell proliferation [20, 21]. Moreover, different studies suggested that 3-substituted chromones and coumarins are potential scaffolds for the design and synthesis of anticancer agents [22, 23]. In particular, Schiff bases of 3-substituted coumarin have proved to have antioxidant [24], antifungal [25] and anticancer [26] properties. A series of coumarin Schiff bases containing sulfonamide moieties were synthesized and evaluated as cytotoxic agents against B16-F10 (B16 melanoma) and MCF-7 (breast cancer) cell lines [27]. Furthermore, coumarin Schiff bases of phosphorohydrazine were assessed as alkylating agents against L1210 and P388 cell lines of leukemia [28].

In the present study, we synthesized some Schiff bases of 3-acetyl-4-hydroxycoumarin (3-acetyl-4-hydroxy-2*H*-chromen-2-one) as cytotoxic agents and characterized them by means of NMR, IR, MS and elemental analyses. Moreover, to get more insights into the electronic structures of the title compounds together with finding more stable tautomers and conformers, the full geometry optimizations were applied using density functional theory (DFT) calculations. Thus, we report here, the synthesis, characterization, computational studies and cytotoxic activity of coumarin-based imines/enamines **3a**–**o**.

Results and discussion

Chemistry

The synthesis of title compounds **3a**–**o** is illustrated in Fig. 1. 4-Hydroxy-2*H*-chromen-2-one (**1**) was reacted with acetic acid as an acetyl source and solvent in the presence of phosphorus oxychloride to give 3-acetyl compound **2** [29]. Compound **2** as a ketone can react with various amines to form a wide range of anilino or benzylamino derivatives (**3a**–**i** and **3j**–**o**, respectively). All the anilino and benzylamino adducts of 3-acetyl-4-hydroxy-2*H*-chromen-2-one were readily provided in reflux condition in ethanol as solvent without any catalyst. All the compounds were characterized by means of FT-IR, NMR, mass spectroscopy and elemental analyses, and the related data are presented in Experimental section. For clear interpretation of ^{1}H and ^{13}C NMR spectra, the atom numbering of the general structure is illustrated in Fig. 2.

At the first glance, it is expected that the final products from the reaction of anilines or benzylamines with the compound **2** be an imine. However, as depicted in Fig. 1, the imine prototype can exist as (*s-cis*)-imine or *s-trans* forms. Further tautomeric transformation of each imine form results in (*E*)- or (*Z*)-enamines with an intramolecular hydrogen bond between NH and carbonyl group of either ketone or lactone functional group. Based on the obtained data from ^{1}H NMR and FT-IR in some cases, we suspected that the final products are preferentially in the enamine form. In particular, in the ^{1}H NMR spectra of benzyl compounds **3k**, **3m** and **3n**, the benzylic CH_2 was split into a doublet by coupling with NH group. Furthermore, the wave number of ketone functional group in **3** was much lower than that of normal ones, which is mainly due to the hydrogen bond between this functional group and NH. However, as interpreted in Experimental section, the rest of compounds can exist in both enamine and imine forms, and consequently, we performed the computational study to investigate which one is the predominant form.

Computational study

The structural analysis

In order to identify the most stable forms of imines and enamines among several possibilities, all the geometries were optimized in the solvent media. The optimized structures have resulted in three stable conformers including (*E*)-enamine, (*Z*)-enamine and (*s-cis*)-imine-1 forms as exemplified in Fig. 3 for compound **3a**. Interestingly, the (*s-trans*)-imine and (*s-cis*)-imine-2 forms mostly convert to (*s-cis*)-imine-1 and (*Z*)-enamine counterparts, respectively. Therefore, the equilibrium is toward (*s-cis*)-imine-1 rather than (*s-trans*)-imine, and (*Z*)-enamine is more stable than (*s-cis*)-imine-2.

The thermodynamic parameters of both isomers of enamine (*E* and *Z*) and (*s-cis*)-imine-1 rotamer of imine are reported in Table 1. The values of electronic energy, ΔE, are ($E_E - E_Z$), and also enthalpy and Gibbs free energy (ΔH and ΔG) values are gained from (enamine H/G − imine H/G) energies, which indicate more stability of (*E*)-enamine over (*s-cis*)-imine-1.

For further investigation, the Gibbs free energy (ΔG) and also enthalpy energy (ΔH) of all three structures were determined (Table 1). The calculated values of ΔH and ΔG

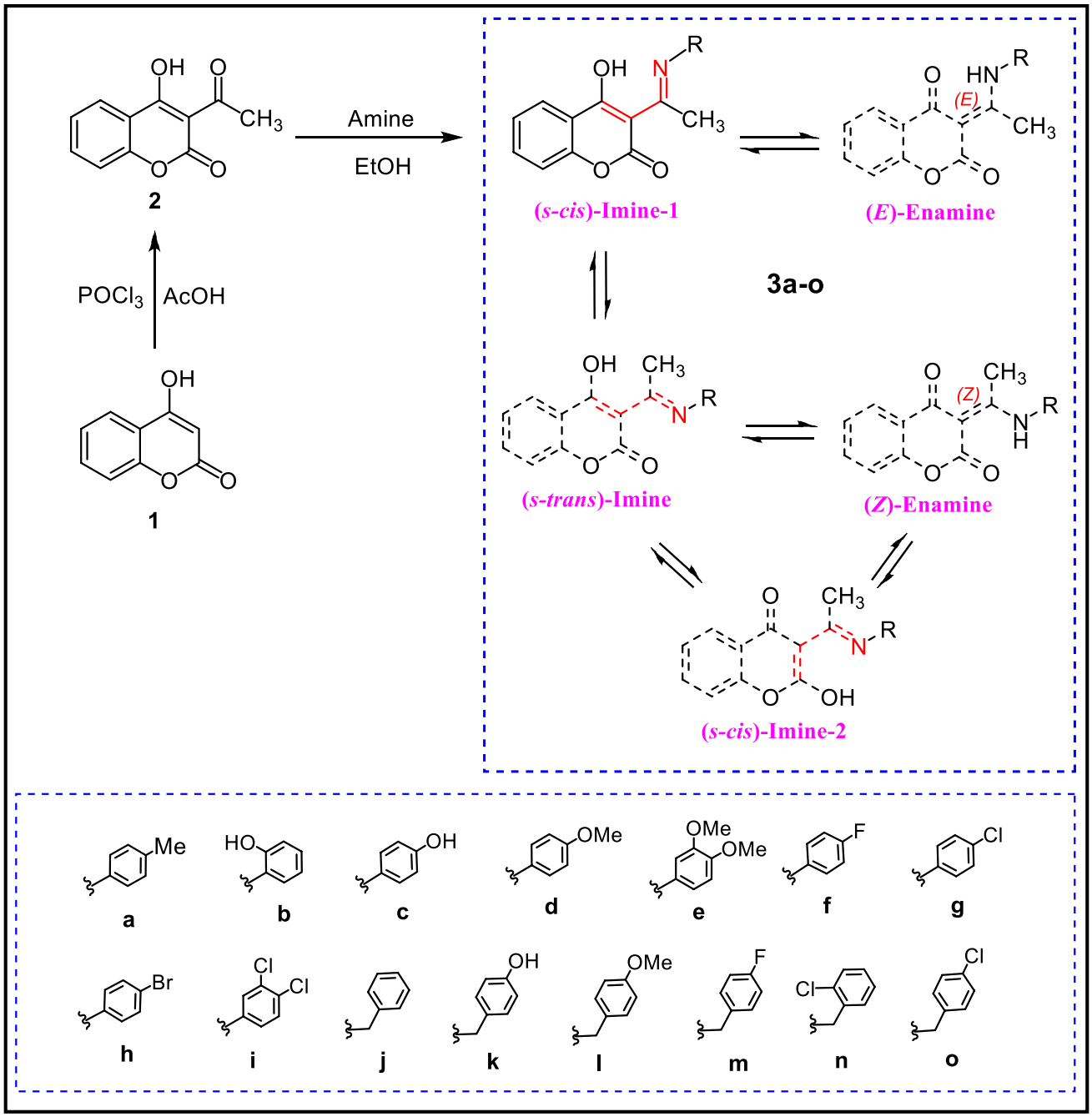

Fig. 1 Synthesis of the anilino and benzylamino adducts of 3-acetyl-4-hydroxy-2*H*-chromen-2-one. The products **3a–o** can exist in different tautomeric forms

are in agreement with ΔE results, indicating the stability of (*E*)-enamine over other isomers. The obtained stability order for the mentioned compounds is: (*E*)-enamine > (*Z*)-enamine > (*s-cis*)-imine-1. The data suggest that the formation of (*E*)-enamine is favorable and more stable than the *Z* ones. The stronger intramolecular hydrogen bond between NH and oxygen of carbonyl group in (*E*)-enamine than hydrogen bond with carbonyl of lactone in (*Z*)-enamine can be responsible for this assumption (Fig. 3). On the other hand, due to the repulsion between electron pairs on adjacent oxygen and nitrogen atoms, the optimization cycles lead to formation of (*s-cis*)-imine-1 conformer rather than *s-trans* conformer in the imine tautomer. In addition, the interaction of hydrogen atoms of the methyl group with the oxygen lone pairs in the (*s-cis*)-imine-1 conformer can lead to the formation of an unconventional C–H…O hydrogen bond [30, 31].

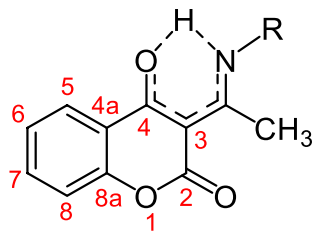

Fig. 2 Atom numbering of the general structure of **3a–o** used for interpretation of ^{1}H and ^{13}C NMR data

To further comprehend the optimized parameters of the three species [(*E*)-enamine, (*Z*)-enamine and (*s-cis*)-imine-1], the critical bond lengths (L1, L2 and L3) and also dihedral angles (D) were computed for all compounds, as defined for compounds **3a** (C=N−C_{arom}=C_{arom} connected atoms) and **3k** (N−CH_2−C_{arom}=C_{arom} connected atoms) in Fig. 4. The obtained values for bond lengths (Å) and dihedral angles (°) of compounds **3a–o** are listed in Table 2. In enamine form of all compounds (**3a–o**), L2 bond possesses features of a double bond rather than a single bond suggesting this bond is shorter when compared with the corresponding bond in imine form. The dihedral angles for aryl derivatives **3a–i** and benzyl analogs **3j–o** were in the range of 47.6–58.5 and 66.9–92.5 degree, respectively (Table 2). To that end, it can be concluded that all the compounds are non-planar. From these observations, imine C=N bond, through tautomeric transformation, turns into NH, which can form the hydrogen bond with the oxygen atom of either ketone or ester functional group.

Moreover, the highest-occupied molecular orbitals (HOMO) and lowest-unoccupied molecular orbitals (LUMO) energies for both imine and enamine due to the importance of frontier orbitals nature in governing chemical reactions or interactions with other species were evaluated by NBO calculations in the solvent media. The band gap energy [E_g ($E_{HOMO} - E_{LUMO}$)] was also calculated which can be used for predicting the most reactive site and also provides explanation for several types of reaction in conjugated systems [32]. The E_g represents the intermolecular charge transfer from an electron donor to electron acceptor group [33]; hence, it can determine the stability, reactivity, polarizability and chemical hardness–softness of different

Table 1 Computational parameters including Δ*E*, Δ*H* and Δ*G* obtained for the synthesized compounds **3a–o**

Compound	Δ*E* (kcal/mol)[a]		Δ*H* (kcal/mol) (*E*)-enamine − (*s-cis*)-imine-1	Δ*G* (kcal/mol) (*E*)-enamine − (*s-cis*)-imine-1
	Enamine ($E_E - E_Z$)	(*E*)-enamine − (*s-cis*)-imine-1		
3a	−1.513	−27.229	−25.516	−22.557
3b	−1.305	−21.528	−21.061	−21.372
3c	−1.530	−27.563	−26.537	−25.208
3d	−1.539	−27.757	−26.915	−22.285
3e	−0.898	−27.348	−25.218	−26.167
3f	−1.543	−26.386	−24.944	−22.666
3g	−1.541	−25.676	−24.255	−21.288
3h	−1.547	−25.66	−23.640	−23.587
3i	−1.617	−24.513	−22.666	−23.240
3j	−0.699	−29.153	−28.377	−27.059
3k	−1.970	−21.692	−24.922	−20.553
3l	−1.925	−29.506	−28.713	−27.833
3m	−1.970	−28.218	−28.223	−24.536
3n	−2.727	−26.286	−25.738	−24.501
3o	−2.039	−27.566	−27.771	−24.747

[a]Energy values calculated in DMSO (as solvent) at room temperature

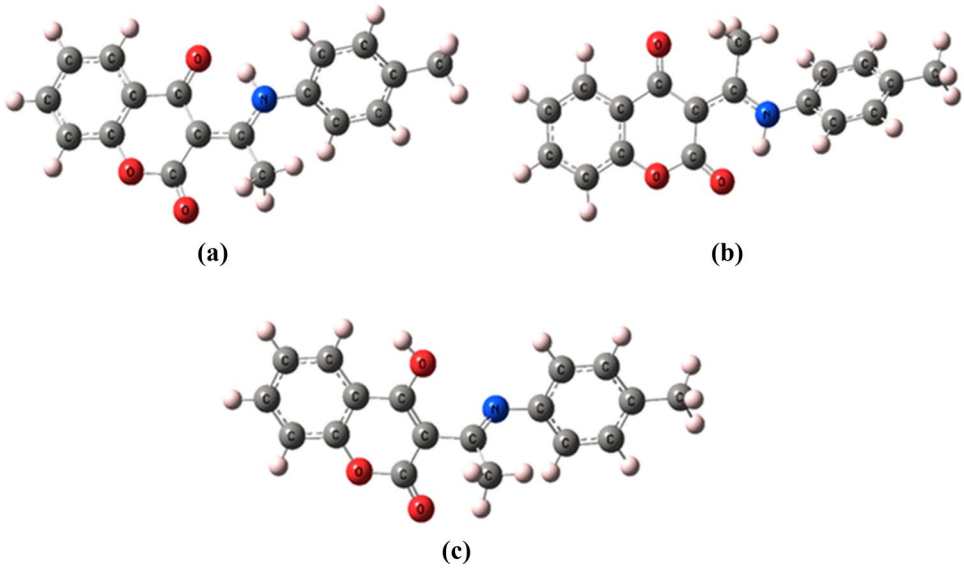

Fig. 3 The optimized structures for compound **3a**: a) (*E*)-enamine; b) (*Z*)-enamine; c) (*s-cis*)-Imine-1

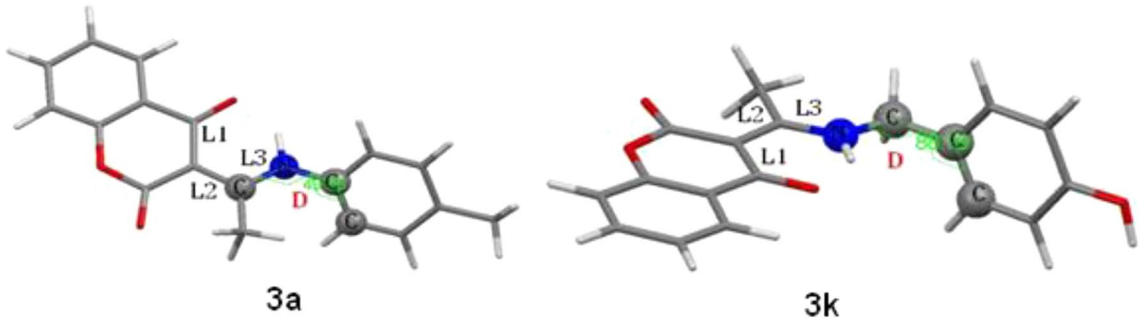

Fig. 4 The bond length (L1, L2 and L3) and dihedral angle (D) schematic of (*E*)-enamine for **3a** (calculated for C=N−C_{arom}=C_{arom}) and **3k** (calculated for N−CH_2−C_{arom}=C_{arom}), as representative compounds

Table 2 The optimized parameters of bond length (Å) and dihedral angles (°) of compounds **3a–o**

No.	Enamine bond length (Å)						(*s-cis*)-Imine-1 bond length (Å)			(*E*)-enamine dihedral angles (°)
	E			*Z*						
	L1	L2	L3	L1	L2	L3	L1	L2	L3	D
3a	1.457	1.424	1.340	1.469	1.423	1.342	1.368	1.502	1.278	49.85
3b	1.456	1.421	1.344	1.471	1.418	1.348	1.375	1.492	1.285	58.52
3c	1.456	1.425	1.339	1.468	1.423	1.341	1.369	1.501	1.279	52.22
3d	1.456	1.425	1.339	1.468	1.424	1.341	1.369	1.501	1.279	52.15
3e	1.457	1.425	1.340	1.468	1.424	1.341	1.368	1.501	1.278	49.59
3f	1.458	1.423	1.341	1.469	1.421	1.343	1.369	1.501	1.278	51.10
3g	1.458	1.422	1.342	1.470	1.420	1.344	1.368	1.501	1.278	48.55
3h	1.458	1.422	1.342	1.470	1.420	1.345	1.368	1.501	1.278	48.24
3i	1.459	1.420	1.344	1.471	1.419	1.347	1.369	1.500	1.278	47.56
3j	1.456	1.426	1.333	1.466	1.425	1.334	1.368	1.505	1.275	89.57
3k	1.456	1.427	1.332	1.466	1.425	1.334	1.371	1.502	1.277	88.80
3l	1.456	1.427	1.332	1.465	1.426	1.333	1.371	1.495	1.278	92.53
3m	1.457	1.426	1.333	1.466	1.424	1.335	1.371	1.495	1.278	89.50
3n	1.457	1.426	1.334	1.468	1.425	1.335	1.371	1.495	1.278	66.89
3o	1.457	1.425	1.334	1.466	1.424	1.335	1.371	1.495	1.278	89.42

chemicals. To that end, enamines of **3a–o** in (*E*)-form are more stable that the other isomers due to the larger energy gap. Moreover, the (*s-cis*)-imine-1 forms of **3a–o** are soft molecules due to smaller E_g which is why they undergo tautomeric transformation (Table 3). The HOMO and LUMO contours of **3a** at 0.02 au are shown in Fig. 5 as an example.

Besides, to investigate the possibility of hydrogen bonding in enamine tautomers and imine conformers, the Mulliken atomic charges for oxygen atoms [of ketone functional group in (*E*)-enamine and hydroxyl in (*s-cis*)-imine-1], nitrogen atom [of amine in (*E*)-enamine and (*s-cis*)-imine-1] and hydrogen atom [of amine in (*E*)-enamine and hydroxyl in (*s-cis*)-imine-1] were calculated by NPA analysis. The obtained results confirmed the feasibility of formation of hydrogen bond in (*E*)-enamine and (*s-cis*)-imine-1; however, due to the larger negative charge of ketone functional group in (*E*)-enamine in comparison with nitrogen atom in (*s-cis*)-imine-1, hydrogen bonding is more favorable in (*E*)-enamine (Table 3).

The molecular electrostatic potential (MEP) surfaces of the studied structures are shown in Fig. 6. As it is shown, MEP can be related to electron density and indicates electrophilic or nucleophilic properties of different sites throughout the whole molecule. Figure 6 shows MEP of **3a** as an example, in which the imine forms obviously hold positive charge at their hydroxyl group and also negative charge at their lactone group, while the enamine ones possess negative charge at their lactone and ketone groups.

Table 3 Band gap energy (E_g) calculation and Mulliken atomic charge for compounds **3a–o**

Compound	E_g (eV)			Mulliken atomic charge					
	Enamine		Imine	(*E*)-enamine			(*s-cis*)-imine-1		
	E	*Z*	*s-cis*	O	H	N	O	H	N
3a	−4.3485	−4.228	−3.960	−0.591	0.406	−0.715	−0.608	0.426	−0.455
3b	−4.3977	−4.202	−3.547	−0.598	0.418	−0.749	−0.615	0.427	−0.555
3c	−4.2097	−4.078	−3.709	−0.592	0.405	−0.714	−0.607	0.425	−0.462
3d	−4.1743	−4.044	−3.680	−0.592	0.405	−0.714	−0.607	0.425	−0.461
3e	−4.1014	−4.017	−3.756	−0.593	0.405	−0.719	−0.609	0.424	−0.461
3f	−4.4070	−4.279	−4.057	−0.590	0.407	−0.717	−0.608	0.426	−0.456
3g	−4.3645	−4.251	−4.138	−0.590	0.408	−0.720	−0.609	0.427	−0.453
3h	−4.3400	−4.227	−4.110	−0.590	0.408	−0.721	−0.604	0.427	−0.465
3i	−4.3539	−4.258	−4.272	−0.588	0.410	−0.724	−0.609	0.429	−0.451
3j	−4.7142	−4.590	−4.589	−0.586	0.408	−0.623	−0.611	0.426	−0.400
3k	−4.6103	−4.504	−3.829	−0.587	0.411	−0.621	−0.607	0.432	−0.450
3l	−4.5439	−4.439	−3.937	−0.586	0.407	−0.621	−0.604	0.423	−0.400
3m	−4.7148	−4.588	−4.431	−0.587	0.407	−0.623	−0.604	0.423	−0.405
3n	−4.7224	−4.594	−4.535	−0.588	0.416	−0.604	−0.604	0.423	−0.409
3o	−4.7148	−4.588	−4.478	−0.587	0.408	−0.625	−0.605	0.424	−0.406

Natural bond orbital analysis of (*E*)- and (*Z*)-enamines

The natural bond orbital (NBO) analysis of *E* and *Z* isomers of *N*-benzyl enamines (**3k–o**) was performed at B3LYP/6–31G(d) level. Hydrogen bond forms due to the interaction of the donor lone pair atoms (LP) and the acceptor antibonding orbitals (BD*). The strength of such interaction can be evaluated with *E*(2). We investigated interaction of C=O···HN, to evaluate the stability of (*E*)- and (*Z*)-enamine isomers. The *E*(2) values of (*E*)-enamines are greater than those of (*Z*)-enamines (Table 4), suggesting that the intramolecular electrostatic hydrogen bond interaction in the (*E*)-forms is higher than that of the (*Z*)-ones (Fig. 7).

In summary, the computational data suggest that the (*E*)-enamine form is more stable than (*Z*)-enamine. This may be due to the higher electron density of ketone carbonyl in comparison with lactone carbonyl, which leads to stronger hydrogen bond with NH. Furthermore, the (*s-cis*)-imine-1 is rapidly converted to (*E*)-enamine form due to the prompt transition of a proton from OH to nitrogen atom regarding to the higher basic nature of N atom.

Cytotoxic activity

All the synthesized compounds **3a–o** were evaluated in vitro for their cytotoxic activities against two cancer cell lines including MCF-7 (breast cancer cell line) and A549 (adenocarcinomic human alveolar basal epithelial cells) and a normal cell line namely BEAS-2B (human normal bronchial epithelium cell line) using MTT assay. Doxorubicin (an antitumor agent) was used as the standard drug. Furthermore, the parent compound **2** was included in cytotoxic assay for comparison. The obtained IC_{50} values are listed in Table 5.

As evidenced from data, most of the compounds showed significant cytotoxic activity against cancer cell lines with IC_{50} values in the range of 1.41–50.0 µg/mL. While the parent carbonyl compound (**2**) showed mild activity against A549 cells (IC_{50} = 29.75 µg/mL), the aniline-derived compounds **3d** and **3h**, and benzyl amine derivatives **3k**, **3m** and **3o** had IC_{50} values less than 10 µg/mL, exhibiting better activities. Among them, **3k** and **3m** displayed the most cytotoxic activity against A549, with IC_{50} values of 6.08 and 6.29 µg/mL, respectively. Compounds **3a**, **3d** and **3k–n** had IC_{50}s < 5 µg/mL, showing high activity against MCF-7 superior to that of doxorubicin (8.87 µg/mL). In particular, the activity of **3k** was sixfold greater than that of doxorubicin against MCF-7. Furthermore, all compounds with the exception of **3b**, **3c**, **3 h** and **3i** were significantly more potent than parent compound **2** against MCF-7 cell line.

The cytotoxicity evaluation against normal cell line BEAS-2B revealed that doxorubicin had no selectivity for cancer cells as its IC_{50} values against cancer cells were close to the value toward normal cell line. On the other hand, the mother coumarin **2** showed equal toxicity against normal and cancer cell lines. The comparison of the IC_{50} values against MCF-7 and BEAS-2B cell lines indicated that compounds **3a**, **3d**, **3k** and **3m–o** display significant selectivity toward MCF-7 to some extent. However, most of the compounds showed low or no selectivity against A549 over BEAS-2B. It is worth to note that compound **3o** displayed high toxicity

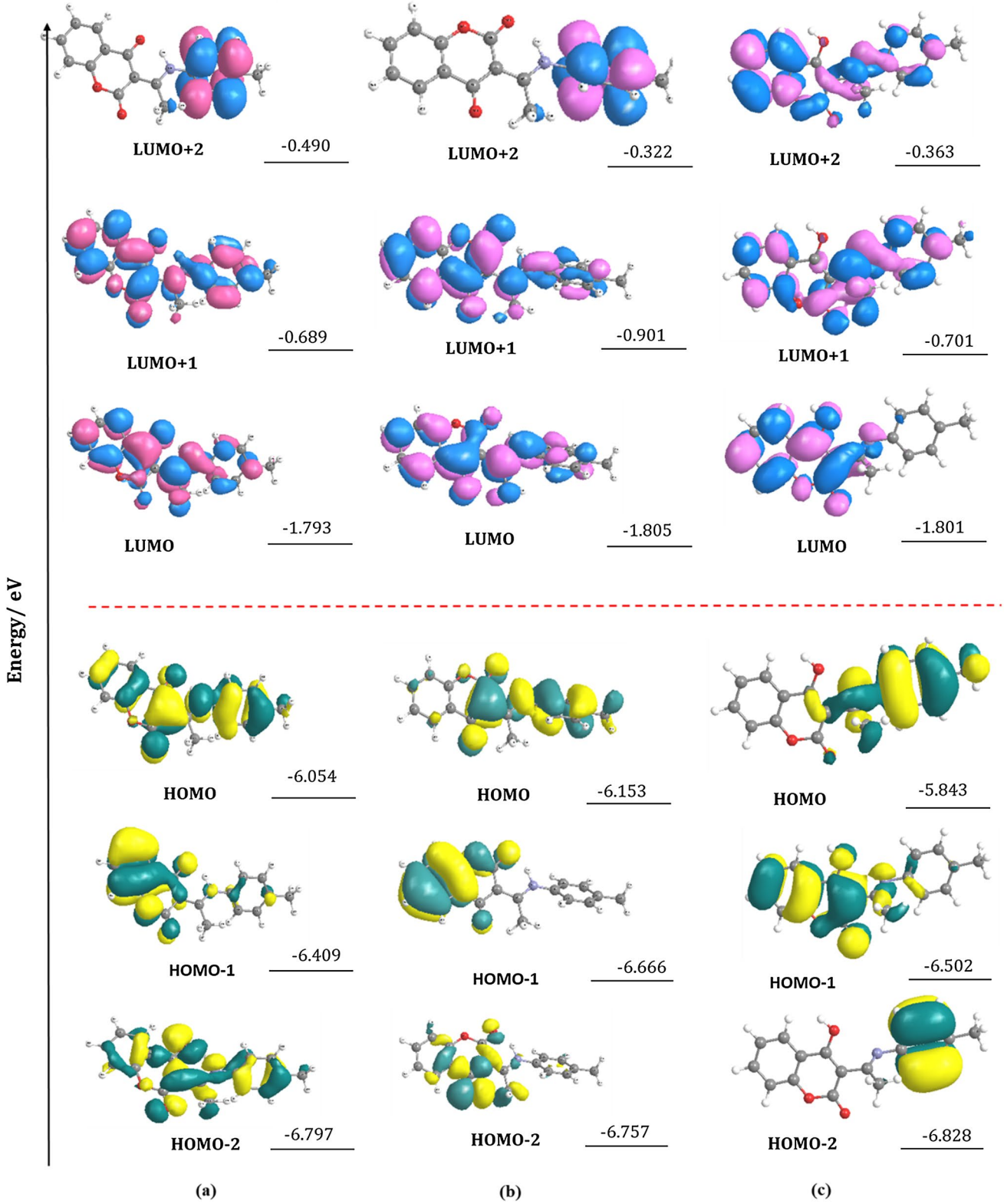

Fig. 5 The energy (eV) and some contours of HOMO and LUMO orbitals of **3a**; (*E*)-enamine (a), (*Z*)-enamine (b) and (*s-cis*)-imine-1 (c). Positive values of the HOMOs and LUMOs contour are represented in green and pink and the negative values in yellow and blue color, respectively

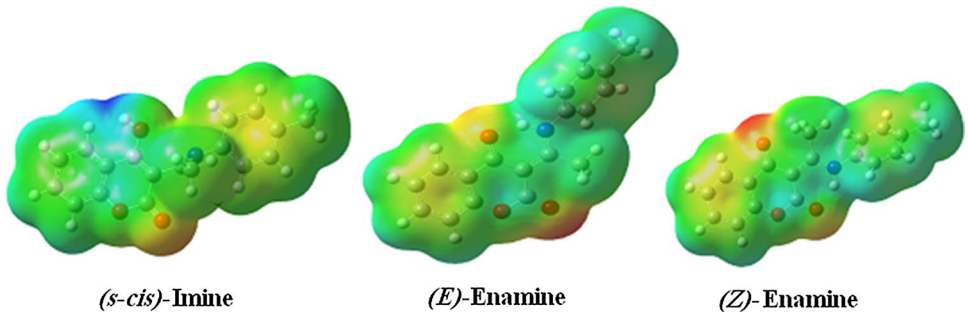

Fig. 6 Calculated molecular electrostatic potential surfaces (MEP) for imine and enamine forms (**3a** is presented as an example). The surfaces are defined by the 0.0004 electrons/b3 contour of the electron density. Color ranges, in au (blue, is more positive than 0.050; red is more negative than −0.050 and green is neutral)

Table 4 NBO analysis of (*E* and *Z*)-enamines of **3k–o** by DFT method B3LYP/6-31G(d)

Compound	Donor(i)	Type	Acceptor(j)	Type	*E*(2) kcal/mol	*E*(j)–*E*(i) (a.u.)	F(i,j) (a.u.)
(*E*)-**3k**	O	LP	N–H	σ*	20.35	0.72	0.110
(*E*)-**3l**	O	LP	N–H	σ*	20.36	0.72	0.110
(*E*)-**3m**	O	LP	N–H	σ*	20.84	0.72	0.111
(*E*)-**3n**	O	LP	N–H	σ*	21.12	0.72	0.112
(*E*)-**3o**	O	LP	N–H	σ*	21.00	0.72	0.111
(*Z*)-**3k**	O	LP	N–H	σ*	17.24	0.72	0.102
(*Z*)-**3l**	O	LP	N–H	σ*	17.10	0.72	0.102
(*Z*)-**3m**	O	LP	N–H	σ*	17.71	0.72	0.103
(*Z*)-**3n**	O	LP	N–H	σ*	19.86	0.72	0.109
(*Z*)-**3o**	O	LP	N–H	σ*	17.93	0.72	0.104

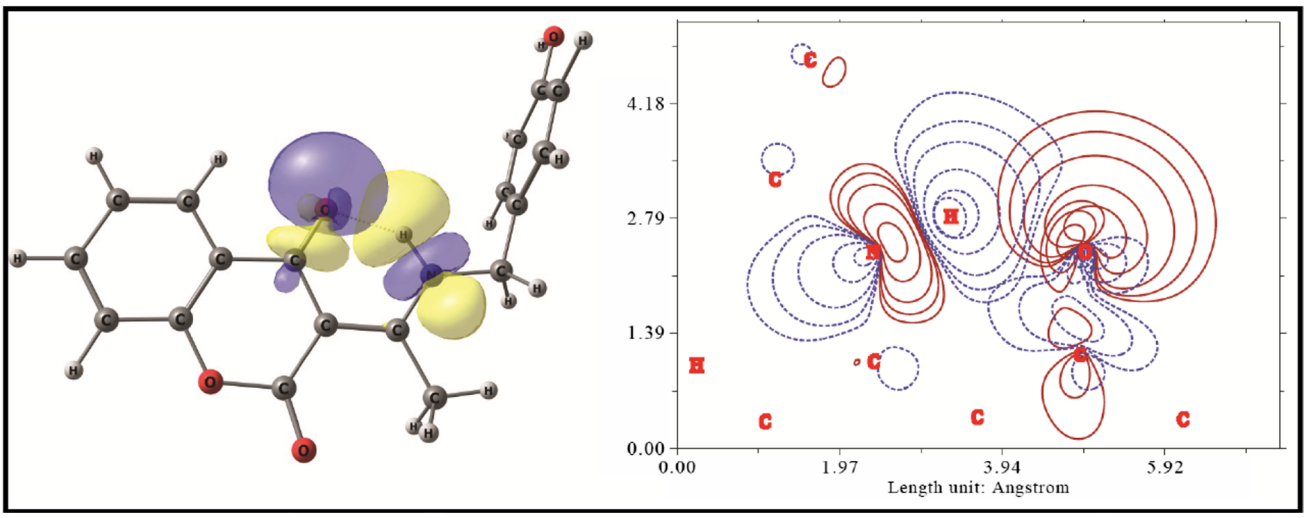

Fig. 7 NBO analysis of (*E*)-enamine for **3k**

against A549 and MCF-7 (IC_{50} value of 8.26 and 7.56 µg/mL) which are very close to those of doxorubicin, while its toxicity against the normal cell line was far more lower than that of doxorubicin.

The structure–activity study of the synthesized compounds demonstrated that the transformation of ketone in compound **2** to imine/enamine significantly increases the cytotoxic activity. In general, the substituted benzyl amino derivatives were more potent than substituted aniline analogs. For example, the 4-HO–Bn (**3k**), 4-F–Bn (**3m**) and 4-Cl–Bn (**3o**) derivatives showed higher activity against cancer cells compared to their corresponding anilino congeners **3c**, **3f** and **3g**, respectively. In the anilino series, better activities were observed with 4-MeO and 4-Br substituents against A549, while 4-MeO and 4-Me groups had more positive effect on activity toward MCF-7. Among the halogenated anilines **3f–i**, the 4-bromo compound (**3h**) showed better activity on A549 cells and 4-fluoro-derivative (**3f**) exhibited higher activity against MCF-7 cell line. The

Table 5 Cytotoxicity (IC_{50}, μg/mL) of synthesized compounds against different cell lines

Compound	R	A549	MCF -7	BEAS-2B
3a	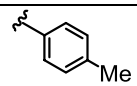	14.28	1.93	10.43
3b		11.07	> 50	> 50
3c	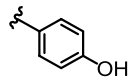	49.98	37.57	22.82
3d	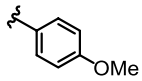	7.66	3.03	13.89
3e	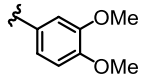	15.25	27.80	23.87
3f	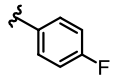	24.56	6.52	13.55
3g	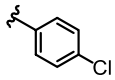	40.00	27.35	46.07
3h	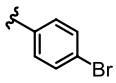	6.84	> 50	8.54
3i	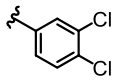	37.20	41.07	> 50
3j	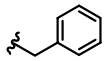	35.28	12.46	10.15
3k	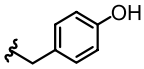	6.09	1.41	4.08
3l	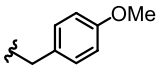	9.35	4.55	2.06
3m	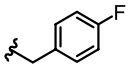	6.29	2.03	4.05
3n	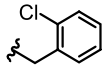	10.74	3.02	35.33
3o	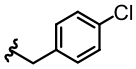	8.26	7.56	> 50
2	–	29.75	32.65	28.81
Doxorubicin	–	5.95	8.87	4.08

Each experiment was conducted in triplicate, and the IC_{50} values were presented as mean

effect of halogen substituent depends on the type of cancer cell line. While the 4-hydroxy derivative of aniline (**3c**) was less potent than the 4-methoxy one (**3d**), conversely in benzyl amines, the 4-hydroxy analog (**3k**) was more potent than the 4-methoxy derivative (**3l**). Among the benzyl amine derivatives, better selectivity toward cancer cells was observed with chloro-derivatives.

Conclusion

We have synthesized some imines/enamines **3a**–**o** derived from 3-acetyl-4-hydroxy-2*H*-chromen-2-one with good yields as cytotoxic agents. Due to the different structural possibility including imine (*s-cis* and *s-trans* conformers) and enamine (*E*- and *Z*-stereoisomers) for these compounds, we performed some calculations by applying

DFT/B3LYP-6-31G(d) method. The computational results including optimized geometry parameters, ΔE, ΔG, ΔH, Mulliken atomic charge, HOMO and LUMO energy, and NBO analysis suggested that the (*E*)-enamine is the more favorable tautomeric form. The in vitro evaluation of anticancer activity for **3a**–**o** confirmed that some of these coumarin derivatives have high toxicity against cancer cell lines A549 and MCF-7. The 4-hydroxybenzyl amine derivative **3k** showed the highest activity (IC_{50}s 6.09 and 1.41 μg/mL), being equipotent or more potent than doxorubicin. However, this compound had no selectivity, similar to doxorubicin. Notably, the 4-chlorobenzyl derivative **3o** with remarkable anticancer activity displayed acceptable selectivity toward cancer cells tested.

Experimental

General information

All the materials including reagents and solvents were purchased from Sigma-Aldrich or Merck companies. The materials were used without further purification unless otherwise stated. The progress and completion of reactions were monitored by TLC using pre-coated silica gel 60 F254 aluminum sheets. The compound spots on TLC were visualized using a UV lamp (254 nm). Melting points were determined in open capillary tubes by a Bibby Stuart Scientific SMP3 apparatus (Stuart Scientific, Stone, UK), and the uncorrected values are reported. Bruker 400 spectrometer was used to record the NMR spectra, and the values were expressed as δ (ppm). The coupling constants are reported in hertz (Hz), and multiplicity was defined as singlet (s), doublet (d), triplet (t) or multiplet (m). Moreover, a HP 5937 Mass Selective Detector (Agilent Technologies, CA, USA) was used to obtain the mass spectra of compounds.

Preparation of 3-acetyl-4-hydroxy-2*H*-chromen-2-one (2)

Compound **2** was synthesized according to the previously reported procedure [34]. Briefly, 4-hydroxy-2*H*-chromen-2-one (**1**, 3 g, 18.6 mmol) was dissolved in acetic acid (20 mL) followed by dropwise adding phosphorus oxychloride (5.6 mL) at room temperature. The resulted solution was brought to reflux temperature. After 30 min, an extra phosphorus oxychloride (1 mL) was added to the solution and the solution was refluxed for another 30 min. After cooling, the product was precipitated as a yellow powder. In order to purify the product, it was recrystallized from ethanol which resulted in pure compound **2** as white needle-like crystals. Yield 95% (3.6 g); mp 134–136 °C; ^{1}H NMR (400 MHz, DMSO-d_6) δ: 2.79 (s, 3H, CH_3), 7.30 (d, 1H, $J = 8.4$ Hz, H-8), 7.35 (td, 1H, $J = 7.6$ and 0.8 Hz, H-6), 7.70 (td, 1H, $J = 8.4$ and 1.6 Hz, H-7), 8.05 (dd, 1H, $J = 8.0$ and 1.6 Hz, H-5), 17.76 (s, 1H, OH). ^{13}C NMR (100 MHz, DMSO-d_6) δ: 30.19, 101.93, 115.18, 117.32, 125.27, 125.67, 137.16, 154.63, 159.67, 178.36, 205.97.

General procedure for the synthesis of compounds 3a–o

To a mixture of compound **2** (1 mmol) in absolute ethanol (5 mL) was added appropriate amine (1 mmol). The temperature of reaction mixture was raised until all compounds were fully dissolved. Then, the resulted solution was refluxed and monitored by TLC using ethyl acetate and *n*-hexane (1:3) as the eluent. After completion of the reaction (10–120 min), it was cool down to room temperature and the product was precipitated out as a fine powder. The collected powder was recrystallized from absolute ethanol to give pure corresponding compound **3**.

4-Hydroxy-3-(1-(*p*-tolylimino)ethyl)-2*H*-chromen-2-one or 3-(1-(*p*-tolylamino)ethylidene) chromane-2,4-dione (3a) White powder; yield 98% (292 mg); mp 148–149 °C [35].

4-Hydroxy-3-(1-((2-hydroxyphenyl)imino) ethyl)-2*H*-chromen-2-one or 3-(1-((2-hydroxyphenyl) amino)ethylidene)chromane-2,4-dione (3b) Pale yellow powder; yield 78% (232 mg); mp 237–239 °C; IR (KBr, cm^{-1}) ν_{max}: 3410 (N–H), 3272 (O–H), 3057 (C–H Ar), 2973 (C–H), 1704 (C=O/C=N), 1562 (C=C). ^{1}H NMR (400 MHz, DMSO-d_6) δ: 3.44 (s, 3H, CH_3), 6.95 (t, 1H, $J = 7.6$ Hz, H-5 phenyl), 7.07 (d, 1H, $J = 8.0$ Hz, H-3 phenyl), 7.25–7.42 (m, 4H, H-4 and H-6 phenyl, H-6 and H-8), 7.70 (t, 1H, $J = 8.0$ Hz, H-7), 8.02 (d, 1H, $J = 7.6$ Hz, H-5), 10.40 (s, 1H, OH), 15.25 (br s, 1H, OH/NH). ^{13}C NMR (100 MHz, DMSO-d_6) δ: 20.96, 97.65, 116.85, 116.97, 119.86, 120.33, 123.64, 124.30, 126.26, 127.32, 130.03, 134.90, 151.95, 153.68, 162.06, 176.38, 180.73. MS (m/z, %): 295 (M^+, 21), 280 (100), 187 (15), 160 (20), 134 (28), 121 (37). Anal. Calcd for $C_{17}H_{13}NO_4$: C, 69.15; H, 4.44; N, 4.74. Found: C, 69.07; H, 4.51; N, 4.63.

4-Hydroxy-3-(1-((4-hydroxyphenyl)imino) ethyl)-2*H*-chromen-2-one or 3-(1-((4-hydroxyphenyl) amino)ethylidene)chromane-2,4-dione (3c) Pale yellow powder; yield 80% (236 mg); mp 211–214 °C; IR (KBr, cm^{-1}) ν_{max}: 3236 (C–H Ar), 1682 (C=O), 1608 (C=O/C=N), 1564 (C=C). ^{1}H NMR (400 MHz, DMSO-d_6) δ: 2.59 (s, 3H, CH_3), 6.90 (d, 2H, $J = 8.4$ Hz, H-3 and H-5 phenyl), 7.25 (d,

2H, $J = 8.4$ Hz, H-2 and H-6 phenyl), 7.31 (d, 1H, $J = 8.0$ Hz, H-8), 7.34 (t, 1H, $J = 7.6$ Hz, H-6), 7.69 (t, 1H, $J = 7.6$ Hz, H-7), 8.00 (d, 1H, $J = 7.6$ Hz, H-5), 9.84 (br s, 1H, OH), 15.32 (s, 1H, OH/NH). ^{13}C NMR (100 MHz, DMSO-d_6) δ: 20.88, 97.43, 116.47, 116.86, 120.31, 124.33, 126.23, 127.29, 127.42, 134.91, 153.65, 157.76, 162.08, 176.09, 180.65. MS (m/z, %): 295 (M^+, 100), 278 (21), 202 (31), 187 (53), 125 (50), 123 (40), 109 (21), 93 (13). Anal. Calcd for $C_{17}H_{13}NO_4$: C, 69.15; H, 4.44; N, 4.74. Found: C, 69.11; H, 4.57; N, 4.61.

4-Hydroxy-3-(1-((4-methoxyphenyl)imino)ethyl)-2*H*-chromen-2-one or 3-(1-((4-methoxyphenyl)amino)ethylidene)chromane-2,4-dione (3d) Yellowish green; yield 92% (284 mg); mp 241–242 °C [35].

3-(1-((3,4-Dimethoxyphenyl)imino)ethyl)-4-hydroxy-2*H*-chromen-2-one or 3-(1-((3,4-dimethoxyphenyl)amino)ethylidene)chromane-2,4-dione (3e) White powder; yield 88% (298 mg); mp 203–205 °C; IR (KBr, cm^{-1}) ν_{max}: 3384 (N–H), 3063 (C–H Ar), 2995, 2931, 2843 (C–H), 1698 (C=O), 1606 (C=O/C=N), 1566 (C=C). ^{1}H NMR (400 MHz, $CDCl_3$) δ: 2.72 (s, 3H, CH_3), 3.93 (s, 3H, OCH_3), 3.96 (s, 3H, OCH_3), 6.75 (d, 1H, $J = 1.6$ Hz, H-2 phenyl), 6.81 (dd, 1H, $J = 8.4$ and 1.6 Hz, H-6 phenyl), 6.96 (d, 1H, $J = 8.4$, H-5 phenyl), 7.22–7.37 (m, 2H, H-6 and H-8), 7.61 (t, 1H, $J = 7.6$ Hz, H-7), 8.11 (d, 1H, $J = 8.0$ Hz, H-5), 15.73 (s, 1H, OH/NH). ^{13}C NMR (100 MHz, $CDCl_3$) δ: 20.92, 56.16, 56.18, 97.92, 108.91, 111.27, 116.72, 117.88, 120.16, 123.71, 126.05, 129.06, 134.21, 148.93, 149.65, 153.90, 162.55, 176.30, 181.83. MS (m/z, %): 339 (M^+, 100), 324 (27), 307 (9), 218 (6), 187 (34), 138 (14), 121 (28). Anal. Calcd for $C_{19}H_{17}NO_5$: C, 67.25; H, 5.05; N, 4.13. Found: C, 67.07; H, 5.15; N, 4.08.

3-(1-((4-Fluorophenyl)imino)ethyl)-4-hydroxy-2*H*-chromen-2-one or 3-(1-((4-fluorophenyl)amino)ethylidene)chromane-2,4-dione (3f) Pale white powder; yield 98% (291 mg); mp 148–150 °C; IR (KBr, cm^{-1}) ν_{max}: 3398 (N–H), 3071 (C–H Ar), 2921 (C–H), 1712 (C=O), 1610 (C=O/C=N), 1568 (C=C). ^{1}H NMR (400 MHz, $CDCl_3$) δ: 2.70 (s, 3H, CH_3), 7.15–7.36 (m, 6H, H-2, H-3, H-5 and H-6 phenyl, H-6 and H-8), 7.61 (t, 1H, $J = 8.0$ Hz, H-7), 8.11 (d, 1H, $J = 8.0$ Hz, H-5), 15.87 (s, 1H, OH/NH). MS (m/z, %): 297 (M^+, 100), 282 (26), 202 (11), 187 (61), 136 (22), 121 (43), 95 (26). Anal. Calcd for $C_{17}H_{12}FNO_3$: C, 68.68; H, 4.07; N, 4.71. Found: C, 68.61; H, 4.14; N, 4.77.

3-(1-((4-Chlorophenyl)imino)ethyl)-4-hydroxy-2*H*-chromen-2-one or 3-(1-((4-chlorophenyl)amino)ethylidene)chromane-2,4-dione (3g) Pale yellow powder; yield 70% (219 mg); mp 153–155 °C; IR (KBr, cm^{-1}) ν_{max}: 3411 (N–H), 3053 (C–H Ar), 2900 (C–H), 1718 (C=O), 1609 (C=O/C=N), 1560 (C=C). ^{1}H NMR (400 MHz, $CDCl_3$) δ: 2.72 (s, 3H, CH_3), 7.21 (d, 2H, $J = 8.4$ Hz, H-2 and H-6 phenyl), 7.25–7.36 (m, 2H, H-6 and H-8), 7.50 (d, 2H, $J = 8.0$ Hz, H-3 and H-5 phenyl), 7.62 (t, 1H, $J = 8.0$ Hz, H-7), 8.11 (d, 1H, $J = 7.6$ Hz, H-5), 15.93 (s, 1H, OH/NH). MS (m/z, %): 315 ($[M+2]^+$, 35), 313 (M^+, 100), 296 (20), 187 (81), 121 (56). Anal. Calcd for $C_{17}H_{12}ClNO_3$: C, 65.08; H, 3.86; N, 4.46. Found: C, 65.01; H, 3.91; N, 4.44.

3-(1-((4-Bromophenyl)imino)ethyl)-4-hydroxy-2*H*-chromen-2-one or 3-(1-((4-bromophenyl)amino)ethylidene)chromane-2,4-dione (3h) Pale white powder; yield 73% (260 mg); mp 175–178 °C; IR (KBr, cm^{-1}) ν_{max}: 3399 (N–H), 3087 (C–H Ar), 2900 (C–H), 1708 (C=O), 1609 (C=O/C=N), 1558 (C=C). ^{1}H NMR (400 MHz, $CDCl_3$) δ: 2.70 (s, 3H, CH_3), 7.14 (d, 2H, $J = 8.8$ Hz, H-2 and H-6 phenyl), 7.22–7.35 (m, 2H, H-6 and H-8), 7.59 (t, 1H, $J = 8.4$ Hz, H-7), 7.64 (d, 2H, $J = 8.4$ Hz, H-3 and H-5 phenyl), 8.08 (d, 1H, $J = 7.6$ Hz, H-5), 15.94 (s, 1H, OH/NH). MS (m/z, %): 359 ($[M+2]^+$, 70), 357 (M^+, 72), 342 (18), 277 (41), 187 (100), 121 (59). Anal. Calcd for $C_{17}H_{12}BrNO_3$: C, 57.01; H, 3.38; N, 3.91. Found: C, 56.98; H, 3.49; N, 3.75.

3-(1-((3,4-Dichlorophenyl)imino)ethyl)-4-hydroxy-2*H*-chromen-2-one or 3-(1-((3,4-dichlorophenyl)amino)ethylidene)chromane-2,4-dione (3i) Pale white powder; yield 66% (229 mg); mp 158–160 °C; IR (KBr, cm^{-1}) ν_{max}: 3054 (C–H Ar), 2900 (C–H), 1695 (C=O), 1608 (C=O/C=N), 1564 (C=C). ^{1}H NMR (400 MHz, $CDCl_3$) δ: 2.73 (s, 3H, CH_3), 7.14 (dd, 1H, $J = 8.4$ and 1.6 Hz, H-6 phenyl), 7.25–7.36 (m, H-6 and H-8), 7.41 (d, 1H, $J = 1.6$ Hz, H-2 phenyl), 7.60 (d, 1H, $J = 8.4$ Hz, H-5 phenyl), 7.63 (t, 1H, $J = 8.0$ Hz, H-7), 8.11 (d, 1H, $J = 8.0$ Hz, H-5), 16.07 (s, 1H, OH/NH). ^{13}C NMR (100 MHz, $CDCl_3$) δ: 20.88, 98.44, 116.81, 119.81, 123.88, 125.09, 126.17, 127.65, 131.40, 132.72, 133.88, 134.64, 135.70, 153.94, 162.15, 176.28, 182.24. MS (m/z, %): 351 ($[M+4]^+$, 20), 349 ($[M+2]^+$, 48), 347 (M^+, 70), 346 (M^+-H, 95), 324 (27), 311 (12), 187 (100), 121 (70). Anal. Calcd for $C_{17}H_{11}Cl_2NO_3$: C, 58.64; H, 3.18; N, 4.02. Found: C, 58.59; H, 3.35; N, 3.98.

3-(1-(Benzylimino)ethyl)-4-hydroxy-2*H*-chromen-2-one or 3-(1-(benzylamino)ethylidene)chromane-2,4-dione (3j) Pale yellow powder; yield 85% (249 mg); mp 169–171 °C; IR (KBr, cm^{-1}) ν_{max}: 3385 (N–H), 3100 (C–H Ar), 2927 (C–H), 1699 (C=O), 1607 (C=O/C=N), 1568 (C=C). ^{1}H NMR (400 MHz, DMSO-d_6) δ: 2.72 (s, 3H, CH_3), 4.89 (s, 2H, CH_2 benzyl), 7.23–7.52 (m, 7H benzyl and H-6 and H-8), 7.64 (dt, 1H, $J = 8.8$ and 1.6 Hz, H-7), 7.93 (dd, 1H, $J = 8.0$ and 1.6 Hz, H-5), 14.01 (br s, 1H, OH/NH). MS (m/z, %):

293 (M^+, 100), 202 (18), 106 (87), 91 (100). Anal. Calcd for $C_{18}H_{15}NO_3$: C, 73.71; H, 5.15; N, 4.78. Found: C, 73.88; H, 5.25; N, 4.71.

4-Hydroxy-3-(1-((4-hydroxybenzyl)imino)ethyl)-2*H*-chromen-2-one or 3-(1-((4-hydroxybenzyl)amino)ethylidene)chromane-2,4-dione (3k) Pale yellow powder; yield 70% (216 mg); mp 217–220 °C; IR (KBr, cm^{-1}) ν_{max}: 3232 (O–H), 2930 (C–H), 1669 (C=O), 1607 (C=O/C=N), 1461 (C=C). ^{1}H NMR (400 MHz, DMSO-d_6) δ: 2.72 (s, 3H, CH_3), 4.74 (d, 2H, J = 4.0 Hz, CH_2 benzyl), 6.83 (d, 2H, J = 8.0 Hz, H-3 and H-5 benzyl), 7.20–7.35 (m, 4H, H-2 and H-6 benzyl, H-6 and H-8), 7.63 (t, 1H, J = 8.4 Hz, H-7), 7.91 (d, 1H, J = 7.6 Hz, H-5), 9.50 (br s, 1H, OH/NH), 13.87 (s, 1H, NH). ^{13}C NMR (100 MHz, DMSO-d_6) δ: 19.05, 47.72, 96.64, 116.18, 116.69, 120.58, 124.10, 126.10, 126.29, 129.90, 134.48, 153.5, 157.76, 162.32, 176.25, 180.12. MS (m/z, %): 309 (M^+, 43), 203 (100), 107 (55), 92 (26). Anal. Calcd for $C_{18}H_{15}NO_4$: C, 69.89; H, 4.89; N, 4.53. Found: C, 70.01; H, 4.93; N, 4.48.

4-Hydroxy-3-(1-((4-methoxybenzyl)imino)ethyl)-2*H*-chromen-2-one or 3-(1-((4-methoxybenzyl)amino)ethylidene)chromane-2,4-dione (3l) White powder; yield 90% (270 mg); mp 162–163 °C; IR (KBr, cm^{-1}) ν_{max}: 3414 (N–H), 2921 (C–H), 2890 (C–H), 1708 (C=O), 1607 (C=O/C=N), 1463 (C=C). ^{1}H NMR (400 MHz, DMSO-d_6) δ: 2.72 (s, 3H, CH_3), 3.77 (s, 3H, OCH_3), 4.79 (s, 2H, CH_2), 6.99 (d, 2H, J = 8.4 Hz, H-3 and H-5 benzyl), 7.25 (d, 1H, J = 8.4 Hz, H-8), 7.27 (dt, 1H, J = 8.0 and 0.8 Hz, H-6), 7.36 (d, 2H, J = 8.8 Hz, H-2 and H-6 benzyl), 7.62 (td, 1H, J = 8.4 and 1.6 Hz, H-7), 7.90 (dd, 1H, J = 8.0 and 1.6 Hz, H-5), 13.90 (s, 1H, OH/NH). ^{13}C NMR (100 MHz, DMSO-d_6) δ: 19.04, 47.54, 55.58, 96.68, 114.84, 116.69, 120.57, 124.11, 126.10, 128.14, 129.86, 134.51, 153.50, 159.49, 162.31, 176.40, 180.14. MS (m/z, %): 323 (M^+, 50), 186 (9), 161 (8), 121 (100). Anal. Calcd for $C_{19}H_{17}NO_4$: C, 70.58; H, 5.30; N, 4.33. Found: C, 70.69; H, 5.35; N, 4.31.

3-(1-((4-Fluorobenzyl)imino)ethyl)-4-hydroxy-2*H*-chromen-2-one or 3-(1-((4-fluorobenzyl)amino)ethylidene)chromane-2,4-dione (3m) Pale yellow powder; yield 97% (288 mg); mp 165–167 °C; IR (KBr, cm^{-1}) ν_{max}: 3443 (N–H), 3100 (C–H Ar), 2795 (C–H), 1704 (C=O), 1608 (C=O/C=N), 1511 (C=C). ^{1}H NMR (400 MHz, $CDCl_3$) δ: 2.80 (s, 3H, CH_3), 4.76 (d, 2H, J = 5.2 Hz, CH_2 benzyl), 7.14 (t, 2H, J = 8.4 Hz, H-3 and H-5 benzyl), 7.20–7.42 (m, 4H, H-2, H-6 benzyl, H-6 and H-8), 7.58 (td, 1H, J = 8.4 and 1.6 Hz, H-7), 8.05 (d, 1H, J = 7.6 Hz, H-5), 14.64 (s, 1H, OH/NH). ^{13}C NMR (100 MHz, $CDCl_3$) δ: 18.92, 47.56, 97.57, 116.35 (d, $J_{C,F}$ = 21.0 Hz), 116.63, 120.26, 123.63, 125.99, 129.15 (d, $J_{C,F}$ = 8.0 Hz), 130.70 (d, $J_{C,F}$ = 3.0 Hz), 134.05, 153.77, 162.65 (d, $J_{C,F}$ = 246 Hz), 162.67, 177.02, 181.75. MS (m/z, %): 311 (M^+, 71), 294 (8), 202 (45), 174 (13), 124 (21), 109 (100). Anal. Calcd for $C_{18}H_{14}FNO_3$: C, 69.45; H, 4.53; N, 4.50. Found: C, 69.41; H, 4.58; N, 4.42.

3-(1-((2-Chlorobenzyl)imino)ethyl)-4-hydroxy-2*H*-chromen-2-one or 3-(1-(2-chlorobenzylamino)ethylidene)-3*H*-chromene-2,4-dione (3n) Pale yellow powder; yield 100% (330 mg); mp 154–155 °C; IR (KBr, cm^{-1}) ν_{max}: 3062 (C–H Ar), 2900 (C–H), 1695 (C=O), 1587 (C=O/C=N), 1465 (C=C). ^{1}H NMR (400 MHz, DMSO-d_6) δ: 2.80 (s, 3H, CH_3), 4.86 (d, 2H, J = 5.6 Hz, CH_2 benzyl), 7.20–7.41 (m, 5H, H-4, H-5 and H-6 benzyl, H-6, H-8), 7.45–7.52 (m, 1H, H-3 benzyl), 7.57 (td, 1H, J = 8.0 and 1.6 Hz, H-7), 8.06 (d, 1H, J = 7.6 Hz, 5-H), 14.66 (s, 1H, OH/NH). ^{13}C NMR (100 MHz, DMSO-d_6) δ: 18.83, 45.93, 97.66, 116.61, 120.28, 123.61, 126.04, 127.63, 128.96, 129.92, 130.17, 132.68, 133.40, 134.03, 153.75, 162.68, 177.35, 181.74. MS (m/z, %): 329 ($[M+2]^+$, 10), 327 (M^+, 20), 292 (100), 202 (84), 172 (36), 140 (30), 125 (80), 89 (22). Anal. Calcd for $C_{18}H_{14}ClNO_3$: C, 65.96; H, 4.31; N, 4.27. Found: C, 66.08; H, 4.37; N, 4.22.

3-(1-((4-Chlorobenzyl)imino)ethyl)-4-hydroxy-2*H*-chromen-2-one or 3-(1-(4-chlorobenzylamino)ethylidene)-3*H*-chromene-2,4-dione (3o) Pale yellow powder; yield 97.7% (320 mg); mp 170–172 °C; IR (KBr, cm^{-1}) ν_{max}: 3404 (N–H), 3036 (C–H Ar), 2927 (C–H), 1715 (C=O), 1605 (C=O/C=N), 1550 (C=C). ^{1}H NMR (400 MHz, DMSO-d_6) δ: 2.70 (s, 3H, CH_3), 4.90 (s, 2H, CH_2), 7.27 (d, 1H, J = 7.6 Hz, H-8), 7.29 (t, 1H, J = 7.6 Hz, H-6), 7.46 (d, 2H, J = 8.4 Hz, H-2 and H-6 benzyl), 7.52 (d, 2H, J = 8.4 Hz, H-3 and H-5 benzyl), 7.64 (t, 1H, J = 7.2 Hz, H-7), 7.93 (d, 1H, J = 7.6 Hz, H-5), 13.99 (br s, 1H, OH/NH). ^{13}C NMR (100 MHz, DMSO-d_6) δ: 19.10, 47.20, 96.89, 116.69, 120.52, 124.11, 126.12, 129.42, 130.15, 133.12, 134.55, 135.52, 153.51, 162.26, 176.95, 180.24. MS (m/z, %): 329 (($[M+2]^+$, 28), 327 (M^+, 78), 202 (81), 125 (100). Anal. Calcd for $C_{18}H_{14}ClNO_3$: C, 65.96; H, 4.31; N, 4.27. Found: C, 65.77; H, 4.30; N, 4.33.

Cell culturing and MTT assay

Cell viability was evaluated by MTT assay [36]. Cancer cell lines including MCF-7 (breast cancer cells) and A549 (adenocarcinomic human alveolar basal epithelial cells), and normal cell line BEAS-2B (human bronchial epithelium cells) were provided from Pasture Institute, Iran. RPMI with 10% FBS was applied for cell culturing. Firstly, 10^4 cells were seeded into 96-well plates in 200 μL of RPMI culture medium. Five triplicate wells were set up for each compound for different concentrations. After 24 h, 20 μL of sample

solution (synthetic compound or doxorubicin) was added into the wells and incubated at 37 °C under 5% CO_2 for 48 h. Then, 20 µL MTT solution (0.5 mg/mL) was added into the wells and incubated at 37 °C for additional 4 h in darkness. Finally, the supernatant was removed and formazan crystals were dissolved by 200 µL dimethyl sulfoxide (DMSO, Sigma-Aldrich) and the wells absorbance was measured at 570 nm by a microplate spectrophotometer (Biotek). Finally, the IC_{50} values were calculated with respect to the percentage of inhibition at different concentrations by nonlinear curve fitting.

Computational study

A DFT method was employed to optimize all the structures, using Becke's three-parameter hybrid exchange functional with the Lee–Yang–Parr gradient corrected correlation functional (B3LYP hybrid functional) in Gaussian 09 program suite [37, 38]. All the atoms were described with a split valence Pople basis set plus diffuse functions, 6-31G (d) in the gas phase. In order to investigate the effect of solvents (DMSO and $CHCl_3$), the calculations were carried out by solvation model SMD/6-31G(d) level [39]. Frequency calculations were also performed on the all optimized geometries to ensure that the local minima were found. Natural bond analysis (NBO) was used at the same level of theory to analyze the electronic properties as well as the constitution of the molecular orbital. In order to increase the single point, the tight convergence criterion and ultrafine integral grid were exploited.

Acknowledgements This project was related to the Ph.D. thesis of SV (Department of Chemistry, Science and Research Branch, Islamic Azad University, Tehran, Iran). We thank Dr. Nahid Hasani for her valuable comments and suggestions on the molecular modeling part of our work.

Compliance with ethical standards

Conflict of interest Authors declared no conflicts of interest.

References

1. McGuire S (2016) World cancer report 2014. Geneva, Switzerland: World Health Organization, international agency for research on cancer, WHO Press, 2015. Oxford University Press
2. Stewart B, Wild CP (2014) World cancer report 2014
3. Kondagunta GV, Motzer RJ (2006) Chemotherapy for advanced germ cell tumors. J Clin Oncol 24(35):5493–5502
4. Kayl AE, Meyers CA (2006) Side-effects of chemotherapy and quality of life in ovarian and breast cancer patients. Curr Opin Obstet Gynecol 18(1):24–28
5. Oun R, Moussa YE, Wheate NJ (2018) The side effects of platinum-based chemotherapy drugs: a review for chemists. Dalton Trans 47(19):6645–6653
6. Thomas V, Giles D, Basavarajaswamy GPM, Das AK, Patel A (2017) Coumarin derivatives as anti-inflammatory and anticancer agents. Anticancer Agents Med Chem 17(3):415–423. https://doi.org/10.2174/1871520616666160902094739
7. Xi GL, Liu ZQ (2015) Coumarin-fused coumarin: antioxidant story from N, N-dimethylamino and hydroxyl groups. J Agric Food Chem 63(13):3516–3523. https://doi.org/10.1021/acs.jafc.5b00399
8. Alonso-Castro AJ, Guzman-Gutierrez SL, Betancourt CA, Gasca-Martinez D, Alvarez-Martinez KL, Perez-Nicolas M, Espitia-Pinzon CI, Reyes-Chilpa R (2018) Antinociceptive, anti-inflammatory, and central nervous system (CNS) effects of the natural coumarin soulattrolide. Drug Dev Res 79(7):332–338. https://doi.org/10.1002/ddr.21471
9. Tian D, Wang F, Duan M, Cao L, Zhang Y, Yao X, Tang J (2019) Coumarin analogues from the *Citrus grandis* (L.) osbeck and their hepatoprotective activity. J Agric Food Chem 67(7):1937–1947. https://doi.org/10.1021/acs.jafc.8b06489
10. Kasperkiewicz K, Ponczek MB, Budzisz E (2018) A biological, fluorescence and computational examination of synthetic coumarin derivatives with antithrombotic potential. Pharmacol Rep 70(6):1057–1064. https://doi.org/10.1016/j.pharep.2018.06.002
11. Kontogiorgis C, Nicolotti O, Mangiatordi GF, Tognolini M, Karalaki F, Giorgio C, Patsilinakos A, Carotti A, Hadjipavlou-Litina D, Barocelli E (2015) Studies on the antiplatelet and antithrombotic profile of anti-inflammatory coumarin derivatives. J Enzyme Inhib Med Chem 30(6):925–933. https://doi.org/10.3109/14756366.2014.995180
12. Hassan MZ, Osman H, Ali MA, Ahsan MJ (2016) Therapeutic potential of coumarins as antiviral agents. Eur J Med Chem 123:236–255. https://doi.org/10.1016/j.ejmech.2016.07.056
13. Tang ZH, Liu YB, Ma SG, Li L, Li Y, Jiang JD, Qu J, Yu SS (2016) Antiviral spirotriscoumarins A and B: two pairs of oligomeric coumarin enantiomers with a spirodienone-sesquiterpene skeleton from *Toddalia asiatica*. Org Lett 18(19):5146–5149. https://doi.org/10.1021/acs.orglett.6b02572
14. Emami S, Foroumadi A, Faramarzi MA, Samadi N (2008) Synthesis and antibacterial activity of quinolone-based compounds containing a coumarin moiety. Arch Pharm 341(1):42–48. https://doi.org/10.1002/ardp.200700090
15. Song JL, Yuan Y, Tan HB, Huang RM, Liu HX, Xu ZF, Qiu SX (2017) Anti-inflammatory and antimicrobial coumarins from the stems of Eurya chinensis. J Asian Nat Prod Res 19(3):222–228. https://doi.org/10.1080/10286020.2016.1191474
16. Keri RS, Sasidhar BS, Nagaraja BM, Santos MA (2015) Recent progress in the drug development of coumarin derivatives as potent antituberculosis agents. Eur J Med Chem 100:257–269. https://doi.org/10.1016/j.ejmech.2015.06.017
17. Abdel-Latif MS, Elmeleigy KM, Aly TAA, Khattab MS, Mohamed SM (2017) Pathological and biochemical evaluation of coumarin and chlorophyllin against aflatoxicosis in rat. Exp Toxicol Pathol 69(5):285–291. https://doi.org/10.1016/j.etp.2017.01.014
18. Tejada S, Martorell M, Capo X, Tur JA, Pons A, Sureda A (2017) Coumarin and derivates as lipid lowering agents. Curr Top Med Chem 17(4):391–398
19. Ghanei-Nasab S, Khoobi M, Hadizadeh F, Marjani A, Moradi A, Nadri H, Emami S, Foroumadi A, Shafiee A (2016) Synthesis and anticholinesterase activity of coumarin-3-carboxamides bearing tryptamine moiety. Eur J Med Chem 121:40–46. https://doi.org/10.1016/j.ejmech.2016.05.014
20. Abdel Latif NA, Batran RZ, Khedr MA, Abdalla MM (2016) 3-Substituted-4-hydroxycoumarin as a new scaffold with potent CDK inhibition and promising anticancer effect: synthesis, molecular modeling and QSAR studies. Bioorg Chem 67:116–129. https://doi.org/10.1016/j.bioorg.2016.06.005

21. Li G, Zhang J, Liu Z, Wang Q, Chen Y, Liu M, Li D, Han J, Wang B (2019) Development of a series of 4-hydroxycoumarin platinum(IV) hybrids as antitumor agents: synthesis, biological evaluation and action mechanism investigation. J Inorg Biochem 194:34–43. https://doi.org/10.1016/j.jinorgbio.2019.02.011
22. Emami S, Dadashpour S (2015) Current developments of coumarin-based anti-cancer agents in medicinal chemistry. Eur J Med Chem 102:611–630. https://doi.org/10.1016/j.ejmech.2015.08.033
23. Emami S, Ghanbarimasir Z (2015) Recent advances of chroman-4-one derivatives: synthetic approaches and bioactivities. Eur J Med Chem 93:539–563. https://doi.org/10.1016/j.ejmech.2015.02.048
24. Kotali A, Nasiopoulou DA, Tsoleridis CA, Harris PA, Kontogiorgis CA, Hadjipavlou-Litina DJ (2016) Antioxidant activity of 3-[N-(Acylhydrazono)ethyl]-4-hydroxy-coumarins. Molecules 21(2):138
25. Batran RZ, Khedr MA, Abdel Latif NA, Abd El Aty AA, Shehata AN (2019) Synthesis, homology modeling, molecular docking, dynamics, and antifungal screening of new 4-hydroxycoumarin derivatives as potential chitinase inhibitors. J Mol Struct 1180:260–271. https://doi.org/10.1016/j.molstruc.2018.11.099
26. Bonardi A, Falsini M, Catarzi D, Varano F, Di Cesare Mannelli L, Tenci B, Ghelardini C, Angeli A, Supuran CT, Colotta V (2018) Structural investigations on coumarins leading to chromeno[4,3-c]pyrazol-4-ones and pyrano[4,3-c]pyrazol-4-ones: new scaffolds for the design of the tumor-associated carbonic anhydrase isoforms IX and XII. Eur J Med Chem 146:47–59. https://doi.org/10.1016/j.ejmech.2018.01.033
27. Wang Z-C, Qin Y-J, Wang P-F, Yang Y-A, Wen Q, Zhang X, Qiu H-Y, Duan Y-T, Wang Y-T, Sang Y-L, Zhu H-L (2013) Sulfonamides containing coumarin moieties selectively and potently inhibit carbonic anhydrases II and IX: design, synthesis, inhibitory activity and 3D-QSAR analysis. Eur J Med Chem 66:1–11. https://doi.org/10.1016/j.ejmech.2013.04.035
28. Nawrot-Modranka J, Nawrot E, Graczyk J (2006) In vivo antitumor, in vitro antibacterial activity and alkylating properties of phosphorohydrazine derivatives of coumarin and chromone. Eur J Med Chem 41(11):1301–1309. https://doi.org/10.1016/j.ejmech.2006.06.004
29. Shirodkar S (2012) Synthesis, characterization and antimicrobial activity of some new Schiff's bases derived from 5-acetyl-2, 6-dimethylpyrimidin-4(3H)-one and primary aromatic amines. Asian J Chem 24(12):5833–5836
30. Darugar V, Vakili M, Afzali R, Tayyari SF (2017) Conventional and unconventional intramolecular hydrogen bonding in some beta-diketones. Org Chem Res 3(1):61–72
31. Grabowski SJ (2001) Ab initio calculations on conventional and unconventional hydrogen bonds study of the hydrogen bond strength. J Phys Chem A 105(47):10739–10746. https://doi.org/10.1021/jp011819h
32. Mirzaei M, Hadipour NL (2006) An investigation of hydrogen-bonding effects on the nitrogen and hydrogen electric field gradient and chemical shielding tensors in the 9-methyladenine real crystalline structure: a density functional theory study. J Phys Chem A 110(14):4833–4838. https://doi.org/10.1021/jp0600920
33. Chermette H (1998) Density functional theory: a powerful tool for theoretical studies in coordination chemistry. Coord Chem Rev 178:699–721
34. Vazquez-Rodriguez S, Matos MJ, Santana L, Uriarte E, Borges F, Kachler S, Klotz KN (2013) Chalcone-based derivatives as new scaffolds for hA3 adenosine receptor antagonists. J Pharm Pharmacol 65(5):697–703. https://doi.org/10.1111/jphp.12028
35. Girgaonkar M, Shirodkar S (2012) synthesis, characterization and biological studies of Cu (II) and Ni (II) complexes with new bidentate schiff's base ligands as 4-hydroxy-3-(1-(arylimino) ethyl)(arylimino) ethyl) Chromen-2-one. Res J Recent Sci 1:110–116
36. van Meerloo J, Kaspers GJ, Cloos J (2011) Cell sensitivity assays: the MTT assay. Methods Mol Biol (Clifton, NJ) 731:237–245. https://doi.org/10.1007/978-1-61779-080-5_20
37. Frisch M, Trucks G, Schlegel H, Scuseria G, Robb M, Cheeseman J, Scalmani G, Barone V, Mennucci B, Petersson G (2013) Gaussian 09, Revision D. 01. Gaussian. Inc, Wallingford
38. Zhao Y, Truhlar DG (2008) The M06 suite of density functionals for main group thermochemistry, thermochemical kinetics, noncovalent interactions, excited states, and transition elements: two new functionals and systematic testing of four M06-class functionals and 12 other functionals. Theor Chem Acc 120(1–3):215–241
39. Weigend F, Furche F, Ahlrichs R (2003) Gaussian basis sets of quadruple zeta valence quality for atoms H-Kr. J Chem Phys 119(24):12753–12762

Affiliations

Samaneh Vaseghi[1] · Mohammad Yousefi[2] · Mohammad Shokrzadeh[3] · Zinatossadat Hossaini[4] · Zahra Hosseini-khah[5] · Saeed Emami[6]

[1] Department of Chemistry, Science and Research Branch, Islamic Azad University, Tehran, Iran

[2] Department of Chemistry, Yadegar-e Imam Khomeini Shahr-e Rey Branch, Islamic Azad University, Tehran, Iran

[3] Department of Toxicology and Pharmacology, Faculty of Pharmacy, Mazandaran University of Medical Sciences, Sari, Iran

[4] Department of Chemistry, Qaemshahr Branch, Islamic Azad University, Qaemshahr, Iran

[5] Diabetes Research Center, Mazandaran University of Medical Sciences, Sari, Iran

[6] Department of Medicinal Chemistry and Pharmaceutical Sciences Research Center, Faculty of Pharmacy, Mazandaran University of Medical Sciences, Sari, Iran